CHIN. PHYS. LETT. Vol. 36, No. 3 (2019) 034302

Maximization of Acoustic Levitating Force for a Single-Axis Acoustic Levitation System Using the Finite Element Method *

Saurabh Yadav**, Arpan Gupta

Acoustic and Vibration Laboratory, School of Engineering, Indian Institute of Technology Mandi, Himachal Pradesh 175005, India

(Received 16 November 2018)

We investigate single-axis acoustic levitation using standing waves to levitate particles freely in a medium bounded by a driver and a reflector. The acoustic pressure at the pressure antinode of the standing wave counteracts the downward gravitational force of the levitating object. The optimal relationship between the air gap and the driving frequency leads to resonance and hence maximization of the levitating force. Slight deviation from the exact resonance condition causes a reduction in acoustic pressure at the pressure antinodes. This results in a significant reduction of the levitating force. The driving frequency is kept constant while the air gap is varied for different conditions. The optimal air gap for maximizing the levitation force is studied for first three resonance modes. Furthermore, a levitating particle is introduced between the driver and the reflector. The dependence of the resonance condition on the size of the levitating particle as well as the position of the particle between the driver and the reflector has also been studied. As the size of the levitating particle increases, the resonance condition also gets modified. Finite element results show a good agreement with the validated results available in the literature. Furthermore, the finite element approach is also used to study the variation of acoustic pressure at the pressure antinode with respect to the size of the reflector. The optimum diameter of the reflector is calculated for maximizing the levitating force for three resonance modes.

PACS: 43.10.Df, 43.20.El, 43.35.-c DOI: 10.1088/0256-307X/36/3/034302

Acoustic levitation is an interesting phenomenon with future applications in the field of container-less handling of reactive and toxic materials. In addition to levitating particles, acoustic levitation has also been used to measure different properties of materials such as adiabatic compressibility, density, sound speed and surface tension at normal temperatures[1–4] as well as supercooled temperatures.[5,6] Acoustic levitation has been achieved using the flexural or bending mode vibrations of an annular plate at 20 kHz.[7] Polystyrene balls of several millimeters in diameter have been levitated successfully. Levitation of the highest density solid material (iridium, $\rho = 22.6\,\mathrm{g/cm^3}$), as well as the highest density liquid material (mercury, $\rho = 13.6\,\mathrm{g/cm^3}$), has been achieved using ultrasonic sound waves.[8] Marston[9] provided an improved approximation to calculate the radiation force applied to a sphere in acoustic levitation. A study on handling the microparticles using a sound field has been performed[10] and an acoustic levitation transportation system has been developed to move the particles in a linear direction.[11] The parameters of the single-axis acoustic levitator play an important role in determining the radiation force. Parametric studies have been conducted to enhance the capability of the single-axis acoustic levitation system.[12–14] A single-axis acoustic levitation system uses standing waves to levitate particles. Different methods have been used to study the resonance conditions of single-axis acoustic levitation for a closed chamber.[15,16] The boundary element method has been used to study resonance conditions of open single-axis acoustic levitation systems.[17] The nonlinear behavior of the single-axis acoustic levitator[18] as well as the oscillations of the solid spherical particle between the driver and the reflector[19] have been studied. Andrade *et al.*[20] presented a review of the recent progress in the field of acoustic levitation.

As mentioned in the literature, the levitation force can be improved using the surface of the reflector or driver or both as a curved surface. The size of the reflector can also be a very important parameter to obtain the maximum levitating force. However, to date, this parameter has not been studied. In this Letter, the finite element method is used to study different aspects of a single-axis acoustic levitation system for maximization of the levitating force. The effect of the reflector size on the levitating force is studied and the size of the reflector is calculated for the maximum levitating force for the first three resonance modes.

The single-axis acoustic levitator consists of a driver and a reflector. For finite element analysis, the diameters of the driver and the reflector are taken as 1.5λ and 2λ, respectively (where λ is the wavelength). In this study, the driving frequency is taken as 25 kHz. The reflector surface is taken as a curved surface with a 2λ radius of curvature. These parameters are the same as those used by Xie *et al.*[17] so that the finite element results can be validated with the published results available in the literature.[17] The 2D axis sym-

*Supported by the Science and Engineering Research Board under Grant No YSS/2015/001245.
**Corresponding author. Email: saurabh16yadav@gmail.com

metric model is used due to the symmetry of the geometry about the center axis. Figures 1(a) and 1(b) represent the geometry of the single-axis acoustic levitator without a levitating object and with a levitating object, respectively.

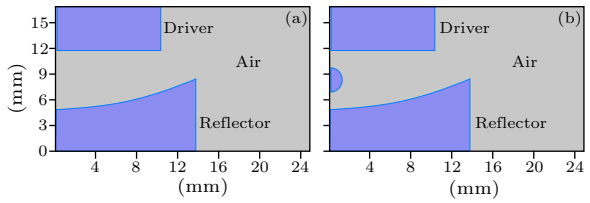

Fig. 1. Geometry of single-axis acoustic levitator (a) without levitating object and (b) with levitating object at the center of the air gap.

When the distance between the driver and the reflector is right, it results in a standing wave on a particular driving frequency. This is known as the resonance condition, which can be achieved in two ways. (1) If H_n (where n represents the resonant mode), i.e. the air gap between the driver and the reflector, is fixed, then the excitation frequency can be adjusted to find out the nth mode resonance condition. (2) If the excitation frequency is fixed, then H_n can be adjusted to find out the nth mode resonance condition. In this work, the second approach is used as the driver is excited harmonically with the excitation frequency of 25 kHz. The value of H_n, at which the resonance occurs, is referred to as the resonance condition. Due to the vibration of the driver surface, the pressure waves are generated in the air domain. The generated pressure waves[21] and their solution are

$$\nabla^2 p = \frac{1}{c_0^2}\frac{\partial^2 p}{\partial t^2}. \tag{1}$$

$$p = P\cos(\omega t)\cos(kz), \tag{2}$$

where c_0, p and P are the speed of sound in the medium, the acoustic pressure perturbation and the pressure amplitude, and $k = \frac{\omega}{c_0}$. The linearized momentum equation (linear Euler's equation) can be written as[20]

$$\rho_0\left[\frac{\partial \boldsymbol{u}}{\partial t}\right] = -\nabla p. \tag{3}$$

From Eqs. (2) and (3), particle velocity ($\boldsymbol{u}$) can be expressed as

$$\boldsymbol{u} = \frac{P}{\rho_0 c_0}\sin(\omega t)\sin(kz)\hat{k}. \tag{4}$$

The expression for the acoustic radiation force or levitating force ($\boldsymbol{F}_{\rm rad}$) on a small sphere in an arbitrary acoustic field was derived by Gor'kov. The expression[20] in terms of the potential of the acoustic radiation force (U) is

$$\boldsymbol{F}_{\rm rad} = -\nabla U, \tag{5}$$

$$U = 2\pi R^3\left[\frac{f_1}{3\rho_0 c_0^2}\langle(p)^2\rangle - \frac{f_2\rho_0}{2}\langle \boldsymbol{u}\cdot\boldsymbol{u}\rangle\right]. \tag{6}$$

If the levitating sphere density is much larger than the air density, then f_1 and f_2 will equal 1.[20] Using Eqs. (2), (4)–(6), the simplified expression of $\boldsymbol{F}_{\rm rad}$ (with the time average over one time period corresponding to the excitation frequency) can be expressed as

$$\boldsymbol{F}_{\rm rad} = \frac{5k\pi P^2 R^3\sin(2kz)}{6\rho_0 c_0^2}\hat{k}. \tag{7}$$

From Eq. (7), the levitating force $\boldsymbol{F}_{\rm rad}$ depends on the square of amplitude of the acoustic pressure. Hence, a higher acoustic pressure will lead to a higher levitating force.

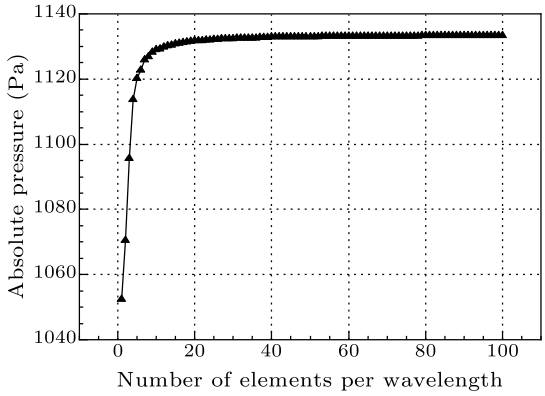

Fig. 2. Convergence plot.

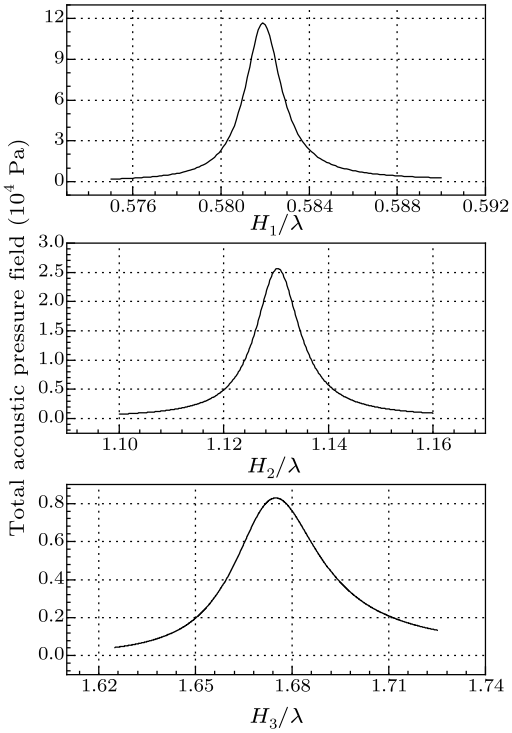

Fig. 3. Plot between the total acoustic pressure field at pressure antinode versus air gap for (a) first, (b) second and (c) third resonance mode.

The finite element analysis software COMSOL Multiphysics is used for this study. The non-reflecting

boundary of the air domain is considered. Thus the plane wave radiation condition is provided to the air domain boundary. The 2D triangular quadratic element (six-noded) is selected for the meshing. The size of the element for the meshing is selected as $\lambda/50$. The solution of the finite element study almost gets converged with this element size. Figure 2 shows the convergence study plot in which the absolute pressure at the center of the geometry is calculated and plotted with respect to the element size.

The driver is excited with the excitation frequency of 25 kHz and the velocity amplitude of 1 m/s. Here H_n is adjusted for the first three modes such that the value of the total acoustic pressure field is at a maximum at the pressure antinodes. These values of H_1, H_2 and H_3 for all three modes are calculated without any levitating particle. Figures 3(a)–3(c) show the total acoustic pressure field with respect to the air gap for all three modes respectively. The peak of these figures represents the resonance.

These finite element values are compared with the values obtained using the boundary element method (BEM).[17] Both values are in very good agreement with each other. The theoretical values ($H_n = \frac{n\lambda}{2}$), BEM values and finite element values of the first three resonance modes are listed in Table 1.

Table 1. Values of the air gap between driver and reflector for the first three resonance modes.

Resonance mode (n)	Air gap for resonance (H_n)	Theoretical value	BEM value[17]	FEM value
1	H_1	0.5λ	0.582λ	0.5819λ
2	H_2	1λ	1.130λ	1.1303λ
3	H_3	1.5λ	1.674λ	1.6749λ

To study the effect of the levitating object on the resonance condition, the levitating object is placed at the center of the air gap between the driver and the reflector. For the first resonance mode, the value of the air gap, i.e. H_1, is calculated and plotted with respect to the particle radius as shown in Fig. 4. There is no significant change under the resonance condition up to the particle radius of 0.025λ. As the radius increases past 0.025λ, the resonance condition starts shifting away. Figures 5(a)–5(c) show the variation of resonance conditions with respect to the size of the levitating particle for all three modes. The finite element results are in good agreement with the results available.[17]

Further, the finite element approach is used to maximize the levitating force by calculating the optimum diameter of the reflector. The radius of curvature of the reflector surface is kept at 2λ. The air gaps for the first, second and third resonances are kept at 0.5819λ, 1.1303λ and 1.6749λ, respectively. The variation of the total acoustic pressure field along the axis of the levitator with varying reflector size is calculated for all three resonance modes as shown in Figs. 6(a)–6(c).

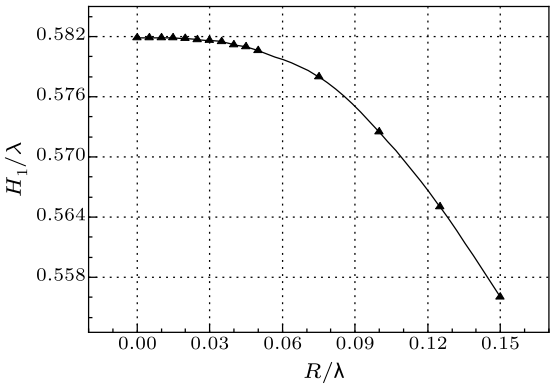

Fig. 4. Variation of resonance condition (air gap, H_1) in first resonance mode with particle size.

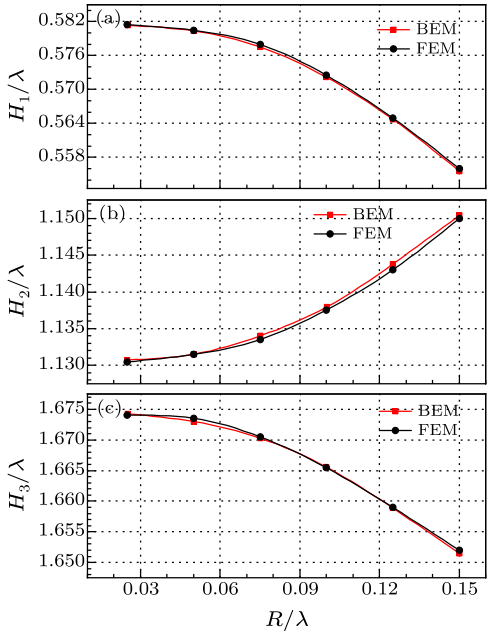

Fig. 5. Change of the resonance condition: (a) H_1, (b) H_2 and (c) H_3 with increasing particle size (R) in first, second and third resonance modes, respectively.

It can be observed from these figures that the total acoustic pressure field changes with the size of the reflector. However, it is difficult to identify the optimum size of the reflector. Thus, the point where the value of the total acoustic pressure field is at its maximum is obtained for all three modes. For the first mode, this point is near the reflector surface. For the second and third modes, it is at 7.615 mm and 15.31 mm from the reflector surface, respectively. The values of the total acoustic pressure field are calculated at these points with a varying diameter of the reflector for all three resonance modes as shown in Figs. 7(a)–7(c), respectively. The optimum values of the reflector diameter for the first, second and third resonance modes are obtained as 2.07λ, 2.19λ and 3.04λ, respectively. As the resonance mode increases, the optimum size of the reflector also increases. It can be understood that the sound waves travel from the flat-surfaced driver and also move away from the axis of the levitator. For a

higher resonance mode, the sound waves become more distributed. Thus a larger size reflector is needed to concentrate the sound waves along the axis of the levitator.

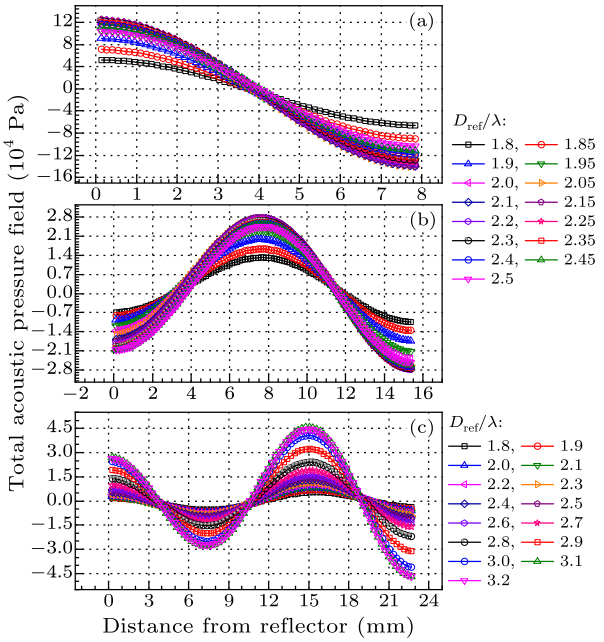

Fig. 6. Pressure profiles along the axis of the levitation system for the (a) first, (b) second and (c) third resonance modes for different diameters of reflector $D_{\rm ref}$.

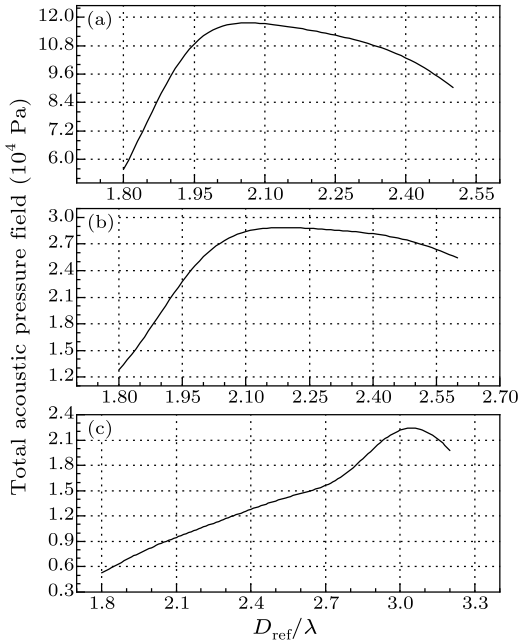

Fig. 7. Variation of maximum total acoustic pressure field with respect to the diameter of the reflector, $D_{\rm ref}$ for the (a) first, (b) second and (c) third resonance modes, respectively.

In summary, the resonance conditions of a single-axis acoustic levitation system for the first three resonance modes are studied using the finite element method. The exact resonance conditions without a levitating object as well as with a levitating object are obtained. The resonance conditions without a levitating object are obtained as 0.5819λ, 1.1303λ and 1.6749λ, respectively. The effects of the spherical levitating object and its size on the resonance conditions are also studied. After 0.025λ, further increases in the particle size result in a significant shift under the resonance condition. The variation of the total acoustic pressure field along the axis of the levitator with respect to the size of the reflector is also studied for the first three resonance modes. Keeping the other parameters fixed (the diameter of the driver as 1.5λ and the radius of curvature of the reflector surface as 2λ), the optimum diameters of the reflector are calculated to be 2.07λ, 2.19λ and 3.04λ for the first, second and third resonance modes, respectively.

References

[1] Apfel R E 1976 *J. Acoust. Soc. Am.* **59** 339
[2] Trinh E H and Hsu C J 1986 *J. Acoust. Soc. Am.* **80** 1757
[3] Tian Y, Holt R G and Apfel R E 1995 *Rev. Sci. Instrum.* **66** 3349
[4] Kremer J, Kilzer A and Petermann M 2018 *Rev. Sci. Instrum.* **89** 015109
[5] Trinh E H and Apfel R E 1980 *J. Chem. Phys.* **72** 6731
[6] Trinh E H and Ohsaka K 1995 *Int. J. Thermophys.* **16** 545
[7] Kandemir M H and Çalışkan M 2016 *J. Sound Vib.* **382** 227
[8] Xie W J , Cao C D, Lü Y J and Wei B B 2002 *Phys. Rev. Lett.* **89** 104304
[9] Marston P L 2017 *J. Acoust. Soc. Am.* **142** 1167
[10] Ostasevicius V, Jurenas V, Gaidys R and Golinka I 2017 *Vibroengineering Procedia.* **15** 100
[11] Thomas G P L, Andrade M A B, Adamowski J C and Silva E C N 2017 *IEEE Trans. Ultrason. Ferroelectr. Freq. Control* **64** 839
[12] Oran W A, Berge L H and Parker H W 1980 *Rev. Sci. Instrum.* **51** 626
[13] Xie W J and Wei B 2001 *Appl. Phys. Lett.* **79** 881
[14] Xie W J and Wei B B 2002 *Phys. Rev. E* **66** 026605
[15] Leung E, Lee C P, Jacobi N and Wang T G 1982 *J. Acoust. Soc. Am.* **72** 615
[16] Santillan A O and Cutanda-Henríquez V 2008 *J. Acoust. Soc. Am.* **124** 2733
[17] Xie W J and Wei B B 2007 *Chin. Phys. Lett.* **24** 135
[18] Andrade M A B, Pérez N and Adamowski J C 2014 *J. Acoust. Soc. Am.* **136** 1518
[19] Andrade M A B, Ramos T S, Okina F T A and Adamowski J C 2014 *Rev. Sci. Instrum.* **85** 045125
[20] Andrade M A B, Pérez N and Adamowski J C 2018 *Braz. J. Phys.* **48** 190
[21] Kinsler L E, Frey A R, Coppens A B and Sanders J V 2000 *Fundam. Acoust.* (New York: John Wiley & Sons Inc.) chap 5 p 119